Optimum Shape Design of Single-Sided Linear Induction Motors Using Response Surface Methodology and Finite-Element Method

Article *in* IEEE Transactions on Magnetics · October 2011

DOI: 10.1109/TMAG.2011.2157995

4 authors, including:

Kyu-Seob Kim
Hanyang University

J.P. Hong
Hanyang University

Optimum Shape Design of Single-Sided Linear Induction Motors Using Response Surface Methodology and Finite-Element Method

Byeong-Hwa Lee[1], Kyu-Seob Kim[1], Jung-Pyo Hong[1], and Jung-Ho Lee[2]

[1]Department of Automotive Engineering, Hanyang University, Seoul 133-791, Korea
[2]Department of Electrical Engineering, Hanbat National University, Dukmyung-Dong Yuseong-Gu, Daejeon 305-719, Korea

This paper deals with finding the optimal ratio of height and length of single-sided linear induction motors using the finite-element method (FEM) for magnetic-field analysis coupled with optimal design methodology. For effective analysis, the FEM is conducted in time harmonic field, which provides steady-state performance with the fundamental components of voltage and current. The ratio of height to length providing the required output power is obtained by response surface methodology and optimal values are presented by the variation in output power. When output power is small, the ratio is high and as the power increases, the ratio shows a converged value. Considering the general application of linear motors, usage of a small ratio can be limiting, however, the shape ratio for the maximum thrust can be identified.

***Index Terms*—Design of experiment (DOE), equivalent magnetic circuit network method, finite-element method (FEM), optimization, response surface methodology (RSM), single-sided linear induction motor (SLIM).**

I. Introduction

SINGLE-SIDED linear induction motor (SLIM) has been developed for use in the industry, transportations, OA/FA equipment, etc., because of the advantages of direct drive and simple structure.

The SLIM is very useful in situations requiring linear motion since it produces thrust directly, so the opportunity for industry application is increased [1], [2]. It is possible to divide linear motors into the following categories according to the application:

1) force machines;
2) power machines;
3) machines.

Force machines are short-duty machines operating at very low speed, and efficiency is not a major consideration with regard to the overall performance. Power machines are often operated at medium or high speed and are continuous-duty machines. They must have high efficiency. Energy machines are short-duty machines and have found applications as accelerators. At present, most linear machines are used in low speeds and standstill applications. As power machines, the shape design of the SLIM is dealt with in this paper.

The optimum design of SLIM is subject to performance constraints as the design changes according to the application. In this paper, the variables of SLIMs for the servo system are optimized using the FEM and response surface methodology (RSM). In order to design SLIMs to have the maximum force density, numerous design variables can be used and optimized. Among design variables, the shape ratio, which is the ratio between stator length and height, is chosen and optimal values for various outputs are determined.

The RSM is used for the experiments, which seeks for the relationship between design variables and response in interest area through statistical fitting methods based on the observed data from the system. The response is generally obtained from real experiments or computer simulations. In the case of rotating machines, research on the ratio of stator and rotor diameter for the maximum torque have been conducted [3], [4]; however, in the case of linear motor, little work has been done.

Therefore, this paper deals with the mover's shape ratio of linear motors. By using the FEM and optimization methodology, the shape ratio providing the maximum output power is presented. The optimization is conducted for various output powers. The maximum output power significantly depending on the shape ratio of mover's width and length is investigated.

II. Analysis Theory

A. Determination of Yoke and Tooth Width

Determination of tooth and yoke thicknesses is important for the maximum output. Therefore, it is essential to determine tooth width and yoke thickness since they are not considered as design variables in this paper. In order to assign reasonable values of tooth and yoke thickness, an equivalent magnetic circuit network is used [4].

In each model, tooth and yoke thicknesses are determined to have the minimum reluctance. Assumptions required in the equivalent magnetic circuit network method are as follows.

1) Permeability of tooth and yoke is constant.
2) End effects are not considered.
3) HT, AL, and slot area are determined in the initial design.
4) Leakage flux is not considered.

Equation (1) shows the total reluctance of a simplified equivalent magnetic circuit. Instead of the total magnetic circuit, a simplified model is used based on the symmetry and periodicity. Since the slot area is predetermined in the initial design, the total reluctance is the function of tooth width x and yoke thickness, consequently, determined by slot area and tooth width. The total reluctance of the simplified model is calculated as the variation of x, and the value providing the minimum reluctance is chosen for each experimental model:

$$\begin{aligned} R_{\text{total}} &= R_{\text{tooth}} + R_{\text{yoke}} \\ &= 2 \times x \cdot L_{\text{st}} / \mu((\text{HT} + \text{SD})/2) \end{aligned}$$

Manuscript received February 21, 2011; revised April 11, 2011; accepted May 15, 2011. Date of current version September 23, 2011. Corresponding author: J.-H. Lee (e-mail: limotor@hanbat.ac.kr).

Color versions of one or more of the figures in this paper are available online at http://ieeexplore.ieee.org.

Digital Object Identifier 10.1109/TMAG.2011.2157995

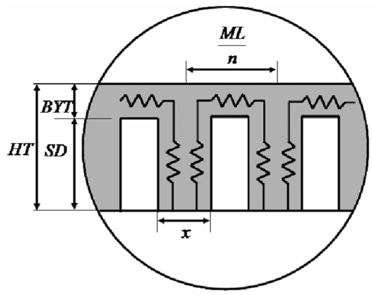

Fig. 1. Equivalent magnetic circuit of mover.

$$+\left((\mathrm{HT}-\mathrm{SD})\cdot L_{\mathrm{st}}/\mu((\mathrm{ML}/n)-x)\right) \quad (1)$$

$$\mathrm{SD}=\text{slot area}/((\mathrm{ML}/n)-x) \quad (2)$$

where R_{total} is the total reluctance, R_{tooth} is the tooth reluctance, R_{yoke} is the yoke reluctance, L_{st} is stack length, μ is the permeability, and x is the tooth width.

B. Optimization

For the optimal design, sampling of experimental data should be conducted initially. In order to do that design of experiment (DOE) is necessary for effective experiments.

Among various DOEs, optimal Latin-hypercube design (OLHD) is used and an approximation is constructed, and then, the progressive quadratic RSM (PQRSM) is used to find an optimal value [5].

1) Design of Experiment: To achieve the optimum design, sampling points are arranged using the OLHD, which is one of many DOE methods [6]. All the axes of factors are arranged by identical numbers using the OLHD.

In other words, all factors are arranged to be on the same level and the axes of factors are equal.

As sampling points are arranged in this way, they may be highly correlated to one another; therefore, sampling points should be evenly distributed by optimum conditions as follows.

As it is not known beforehand that which design will lead to the best performance in terms of $\tilde{\phi}_p$ criterion $(0 \leq \tilde{\phi}_p \leq 1)$ referred to in (3)–(5), one cannot know which design to use.

Fig. 2 shows an example of design for two variables:

$$\phi_p=\left[\sum_{i=1}^{n_p-1}\sum_{j=i+1}^{n_p} d_{ij}^{-p}\right]^{1/p} \quad (3)$$

$$\begin{aligned} d_{ij} &= d(x_i,x_j) \\ &= \left[\sum_{k=1}^{n_\nu}|x_{ik}-x_{jk}|\right]^{1/t}, \quad p=50, t=1 \end{aligned} \quad (4)$$

$$\tilde{\phi}_p=\min(\phi_p)/(\max(\phi_p)-\min(\phi_p)) \quad (5)$$

where n_p is the number of points of the design, and d_{ij} is the interpoint distance between all point pairs in the design, $\max(\phi_p)$ and $\min(\phi_p)$ are the maximum and minimum values found in the generated DOEs.

The OLHD has the advantages in the cases of many design variables. One sampling point being on one level is difficult due to a large number of factors; therefore, sampling points should be spread out evenly by applying optimum conditions. The main effect is obtained by a small number of experiments and the number of sampling points can be set freely [7]. Consequently, the time and the number of experiments can be modified and conducted.

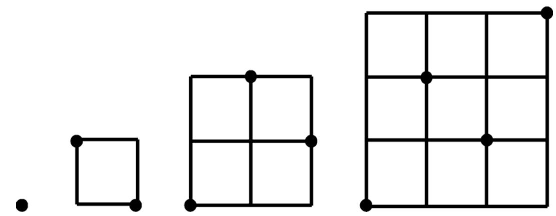

Fig. 2. Example of design for two variables.

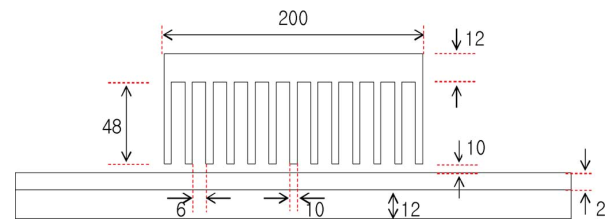

Fig. 3. Dimensions of the initial model.

However, the disadvantage of the OLHD is the difficulty in recognizing correlations between design variables. This is because the level of all the design variables should be identical and interactions between design variables are difficult to figure out. Reappearance is impossible because the sampling point is randomly decided. The number of factors is 3; however, the DOEs is by the application of the OLHD because good results are produced by a smaller number of experiments compared to central composite design (CCD) or full factorial design (FFD). Data processing experiments are conducted ten times for each output.

2) Progressive Quadratic Response Surface Methodology: In this paper, the PQRSM is used, which is one method of the optimum design. The reason is that the conjugated gradient method on the basis of a nonlinear optimum cannot be used.

All of the design parameters are independent. The PQRSM is a method to solve this problem. Just $(2n+1)$ calculations are necessary by choosing $(2n+1)$ sample points to make quadratic approximation functions. And the progressive calculation of rest quadratic terms about interaction by the normalized quasi-Newton method does not need additional calculation [8].

III. Results and Discussion

A. Analysis Model

A 2-pole/12-slot design model is presented in this study. The dimension of an initial model is shown in Fig. 3, and its brief specifications are listed in Table I.

In order to identify the shape ratio according to the output power, five SLIM models were designed, i.e., 250, 375, 500, 625, and 750 W, with constrains of identical pole numbers, slot numbers, winding fill factors, current densities, air gap lengths, etc. Fig. 4 shows the winding configuration of the designed model. The presented winding configuration provides more compact size of the linear motor than the conventional winding presented in [9], but causing undesired high harmonics of current and high thrust force ripples.

By using the FEM and optimization methodology, optimal designs of five SLIMs with different output powers for the maximum power density were obtained. So the optimization

TABLE I
SPECIFICATION OF THE SLIM

	Value
Number of poles	2
Number of phases	3
Number of slots	12
Input voltage	220 V
Frequency	60 Hz
Conductor conductivity	3.12×10^7 S/m
Back iron permeability	0.5×10^7 S/m
Mover material	S23

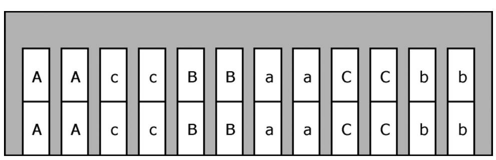

Fig. 4. Winding configuration.

of SLIMs is firstly performed by the objective function and constraint conditions that are defined as follows:

1) Objective function:
   1) thrust force $\geq$23.2N, 91.1N, 151.3N, 205.0N, 323.7N;
2) Constraint conditions:
   mover volume = constant according to output power;
   output power at 250 W, 375 W, 500 W, 625 W, 750 W = constant.

Design variables are given in Fig. 5. Since the tooth width and yoke thickness were determined by using the equivalent magnetic circuit method, first, they are excluded in this optimal design. In addition to ML and HT, thickness of the conductor plate (CT) is added.

Figs. 6 and 7 show the equal potential distribution of the SLIM under the starting and rated condition. It can be found, at starting, that slip is 1 and the main flux does not flow through the CT.

The RSM is applied to make appropriate response models of the thrust force [10]. The polynomial models of the responses are, respectively, given as follows:

$$\begin{aligned}\hat{\mathbf{Y}}_{250\text{ W}} = {} & 0.518 - 0.846X1 + 2.177X2 - 10.644X3 \\ & + 0.004X1^2 + 0.050X2^2 - 29.081X3^2 \\ & - 0.030X1X2 + 1.237X1X3 - 1.606X2X3 \quad (6)\end{aligned}$$

$$\begin{aligned}\hat{\mathbf{Y}}_{375\text{ W}} = {} & -0.447 - 0.026X1 - 2.898X2 + 14.884X3 \\ & + 0.066X2^2 - 40.834X3^2 \\ & - 0.011X1X2 - 0.072X1X3 - 2.84X2X3 \quad (7)\end{aligned}$$

$$\begin{aligned}\hat{\mathbf{Y}}_{500\text{ W}} = {} & -7.763 + 1.519X1 + 0.395X2 - 38.802X3 \\ & - 0.008X1^2 - 0.035X2^2 - 63.008X3^2 \\ & + 0.008X1X2 + 20.766X1X3 - 1.789X2X3 \quad (8)\end{aligned}$$

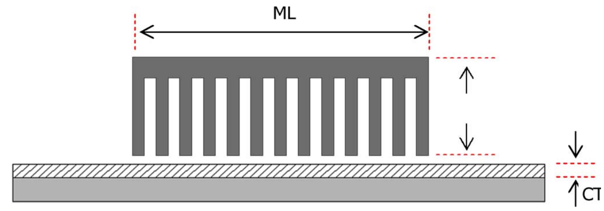

Fig. 5. Variables for the optimal design.

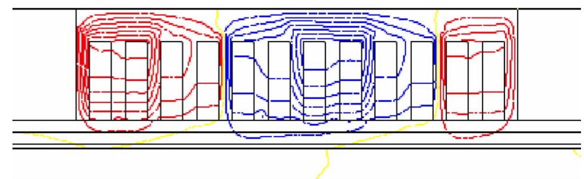

Fig. 6. Equipotentials of Model 3 at starting (slip: 1).

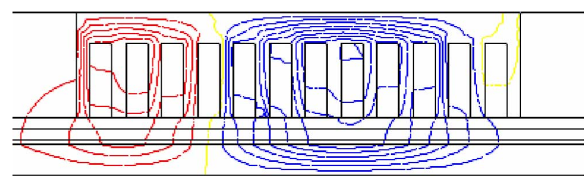

Fig. 7. Equipotentials of Model 3 under the rated condition (slip: 0.2).

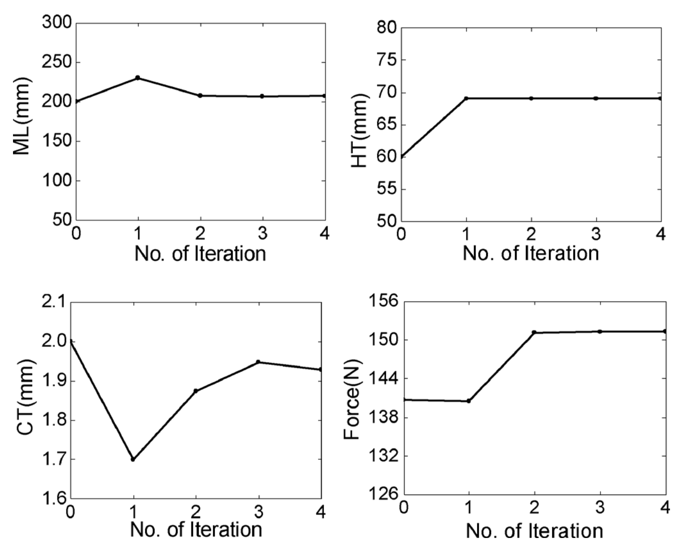

Fig. 8. Converged design variables of the 500-W SLIM.

$$\begin{aligned}\hat{\mathbf{Y}}_{625\text{ W}} = {} & -0.207 + 2.154X1 + 1.151X2 - 2.297X3 \\ & - 0.005X1^2 - 0.031X2^2 - 8.953X3^2 \\ & + 0.007X1X2 - 0.270X1X3 + 0.812X2X3 \quad (9)\end{aligned}$$

$$\begin{aligned}\hat{\mathbf{Y}}_{750\text{ W}} = {} & 1.773 - 0.463X1 + 13.168X2 + 2.799X3 \\ & - 0.008X1^2 - 0.093X2^2 - 30.205X3^2 \\ & - 0.021X1X2 + 0.633X1X3 - 0.916X2X3 \quad (10)\end{aligned}$$

where $X1$ is AL, $X2$ is HT, and $X3$ is CT.

Fig. 8 shows the converged design variables of the 500-W SLIM.

TABLE II
RESULTS OF THE OPTIMUM DESIGN

	AL(mm)	HT(mm)	CT(mm)
250W	115.0	25.5	1.15
375W	172.5	51.8	1.28
500W	207.1	69.0	1.90
625W	227.1	78.3	2.13
750W	255.0	87.5	2.55

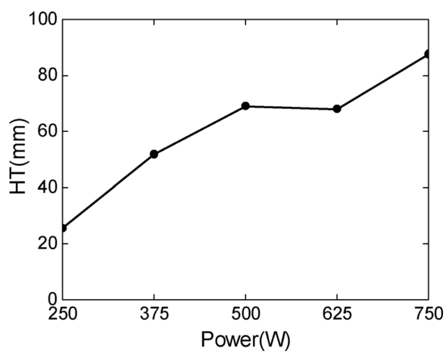

Fig. 9. Determined HT for the output power.

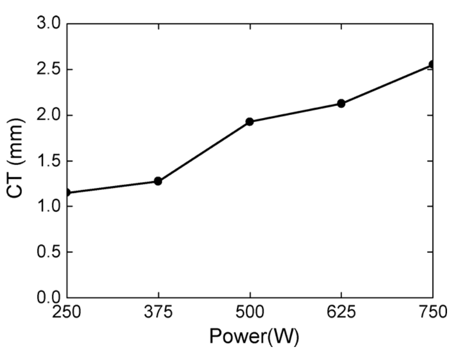

Fig. 10. Determined CT for the output power.

The other SLIMs are optimized by identical process. Design solutions of five SLIMs are listed in Table II.

Figs. 9–11 show the responses of ML, HT, and CT related to the output power increasing. Optimal values of design variables show the proportionality to the output power as shown in Figs. 9–11. For estimating the variation of ML and HT, the ratio of ML and HT is calculated. It is confirmed that as the output power increases, the shape ratio decreases.

Therefore, in the design of the SLIM, appropriate shape ratios should be chosen for maximizing the output power.

IV. Conclusion

The optimal shape ratio of height and length of mover of SLIMs with respect to the output power is determined in this

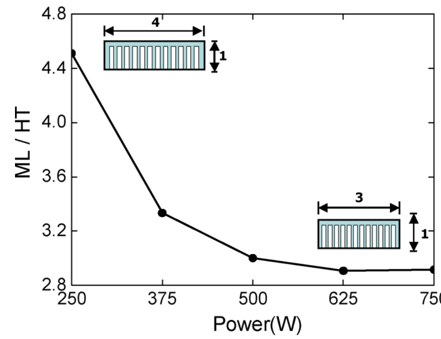

Fig. 11. Shape ratio for the output power.

paper. The results show that as the power becomes larger within a studied range, the shape ratio becomes smaller and converge on 2.9 (ML/HT).

The optimal design result can be restricted due to practical limitations of linear motors. However, the results can be a good reference for the high power density design of the SLIM.

Acknowledgment

This work was supported by Korea Electrical Engineering and Science Research Institute (KESRI) under Grant R-2008-34 funded by the Ministry of Knowledge Economy, Korea, and by the Human Resources Development of the Korea Institute of Energy Technology Evaluation and Planning (KETEP) funded by the Korea Government Ministry of Knowledge Economy under Grant 20104010100600.

References

[1] I. Boldea and S. A. Nasar, *Linear Motion Electromagnetic Systems*. New York: Wiley, 1985.
[2] H.-W. Lee, C.-B. Park, and B.-S. Lee, "Thrust performance of a linear induction motor," *J. Electr. Eng. Technol.*, vol. 6, no. 1, pp. 81–85, 2011.
[3] T. Finken and K. Hameyer, "Design of electric motors for hybrid- and electric-vehicle applications," in *presented at Int. Conf. Electrical Machines Syst.*, Tokyo, Japan, 2009.
[4] T. A. Lipo, *Introduction to AC Machine Design*. Madison, WI: Univ. Wisconsin Press, 1996, vol. 1.
[5] A. Z. Bazghaleh, M. R. Naghashan, and M. R. Meshkatoddini, "Optimum design of single-sided linear induction motors for improved motor performance," *IEEE Trans. Magn.*, vol. 46, no. 11, pp. 3939–3947, Nov. 2010.
[6] X. Liao, X. Yan, W. Xia, and B. Luo, "A fast optimal latin hypercube design for Gaussian process regression modeling," in *Proc. IEEE 3rd Int. Workshop Conf. Adv. Comput. Intell.*, 2010, pp. 474–479.
[7] J.-S. Park, "Optimal latin-hypercube designs for computer experiments," *J. Statist. Plan. Inference*, vol. 39, pp. 95–111, 1994.
[8] S.-J. Yoon and D.-H. Choi, "Air-bearing design based on global approximation concepts," *IEEE Trans. Magn.*, vol. 39, no. 5, pp. 2468–2470, Sep. 2003.
[9] T. Mishima, M. Hiraoka, and T. Nomura, "A study of the optimum stator winding arrangement of LIM in maglev systems," in *IEEE Proc. Electr. Mach. Drives*, 2005, pp. 1238–1242.
[10] S.-I. Kim, J.-P. Hong, Y.-K. Kim, H. Nam, and H.-I. Cho, "Optimal design of slotless-type PMLSM considering multiple responses by response surface methodology," *IEEE Trans. Magn.*, vol. 42, no. 4, pp. 1219–1222, Apr. 2006.